



Biophysical Analysis of CRBN Variants in PROTAC Ternary Kinetics

Comparative Analysis of Full-Length DDB1:CRBN and the Truncated CRBN^{midi} Construct

Abstract

Proteolysis-targeting chimeras (PROTACs) and molecular glues have emerged as powerful therapeutic modalities by exploiting the ubiquitin–proteasome system to drive selective protein degradation. However, structural and biophysical characterization of these degraders is often hampered by the complexity of full-length E3 ligases, particularly cereblon (CRBN), one of the most extensively studied and clinically relevant ligases. CRBN^{midi}, a truncated CRBN construct, overcomes these limitations and enables detailed analysis of degrader-induced ternary complex formation and stability. Here, we compare PROTAC-mediated ternary complexes formed with CRBN^{midi} or the full-length DDB1:CRBN complex in the presence of Brd4 using the **switchSENSE**[®] Y-structure binding assay. Our results demonstrate that CRBN^{midi} forms more stable ternary complexes with slower dissociation kinetics than the full-length E3 ligase. This effect likely arises from the absence of DDB1, which leaves the sensor loop unbound, destabilizes the open state, and favors the closed, ligand-bound conformation. Together, these findings establish CRBN^{midi} as a valuable tool for mechanistic studies and highlight the utility of the DNA Y-structure assay for the characterization and optimization of protein degraders.

Introduction

Targeted protein degradation has emerged as a powerful therapeutic strategy, utilizing small-molecule degraders to harness the ubiquitin–proteasome system for selective elimination of proteins of interest (POIs). Among these degraders, proteolysis-targeting chimeras (PROTACs) are designed to simultaneously recruit an E3 ligase and a POI, initiating ubiquitination and subsequent proteasomal degradation. Cereblon (CRBN) is the most widely employed E3 ligase in PROTAC and molecular glue development, owing to its clinical relevance [1]. Despite its

Keywords:
PROTACs, CRBN^{midi},
CRBN:DDB1, ternary
complex formation,
proximity assay, DNA
Y-structure, **switchSENSE**,
heliX⁺

importance, structure-guided design targeting CRBN has been limited by the scarcity of high-resolution ternary complex structures and biophysical characterization data due to challenging production and handling of the recombinant protein. To overcome these limitations, Kroupova et al. [2] developed CRBN^{mid}, a truncated CRBN construct containing stabilizing mutations that enables high-resolution structural analysis of binary and ternary complexes and facilitates detailed biophysical studies.

Investigating the early steps of degradation – specifically the interactions between PROTACs, E3 ligases, and POIs, as well as the kinetics of ternary complex formation – is essential for the rational selection and optimization of efficient degraders.

To interrogate ternary binding, we developed a proximity-induced, chip-based biosensor assay employing an innovative DNA Y-structure [3]. This nanostructure comprises four DNA strands: two adapter strands carrying distal red and green fluorophores that form the Y-shape, and two DNA–protein conjugated strands that hybridize to the Y-structure, positioning a target protein and the substrate-binding subunit of an E3 ligase at defined 1:1 stoichiometry and proximity (Figure 1). The proteins can swivel freely at the ends of the Y-structure, allowing interactions with each other and with a third molecule, e.g. the bifunctional PROTAC.

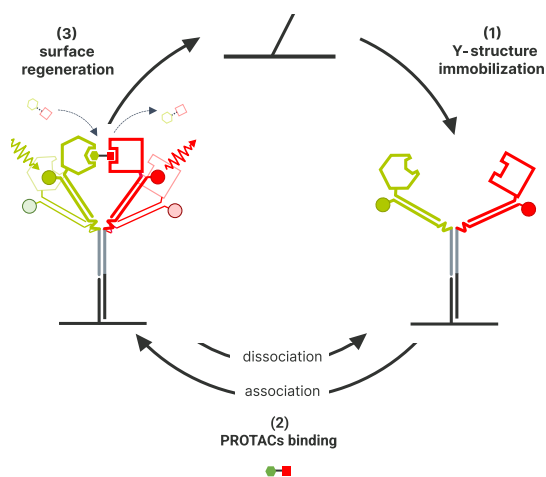


Figure 1. switchSENSE® workflow for PROTAC kinetics study. 1) Immobilization of the Y-structure on the chip surface, pre-mixed with DNA–protein conjugated ligands. 2) Kinetic PROTAC association and dissociation kinetics, with ternary complex formation detected via red FRET signal. 3) Regeneration of the chip surface by injecting a high-pH solution to remove the Y-structure from the chip.

Binary interactions between the PROTAC and either protein are monitored in real time via two-color fluorescence quenching (fluorescence proximity sensing - FPS), while Förster resonance energy transfer (FRET) from the green to the red dye reports ternary complex formation. Unlike traditional surface immobilization methods, the Y-structure does not require pre-incubation step, typical of a classical sandwich assay, and generates a proximity-enhanced environment in which a bifunctional binder engages two connected reactants. The simple switchSENSE® workflow (Figure 1) enables the quantitative measurement of kinetic parameters – association rate (k_{on}), dissociation rate (k_{off}), and affinity (K_d) – for PROTAC-induced ternary complexes. In this study, DDB1:CRBN or CRBN^{mid} were used as the E3 ligase, Brd4^{BD2} as the POI and ARV825, dBET6 and dBET1 as PROTACs. Herein, we demonstrate that CRBN^{mid} forms more stable ternary complexes with slower dissociation kinetics compared to the full-length E3 ligase. This enhanced stability might arise from the CRBN^{mid} sensor loop not being able to bind DDB1, which destabilizes the open conformation and favors the closed, ligand-bound state. Overall, these results underscore CRBN^{mid} as a useful tool for mechanistic studies and highlight the potential of the DNA Y-structure assay to inform rational degrader design.

Materials and Methods

PROTACs ARV825, dBET6, dBET1 (MedChemExpress) were prepared at the indicated concentrations by dilution in HE140 running buffer (10 mM HEPES, 140 mM NaCl, 0.05% Tween-20, 50 μ M EDTA, 50 μ M EGTA; BU-HE-140-10, Dynamic Biosensors GmbH). CRBN^{mid} and Brd4^{BD2} proteins were provided by the Ciulli Lab (University of Dundee). CRBN^{mid} was covalently conjugated via primary amines to the 5' end of ssDNA (Ligand strand 1) using the NHS coupling kit (HK-NYS-NHS-1, Dynamic Biosensors GmbH), and Brd4^{BD2} was coupled to the 3' end of ssDNA (Ligand strand 2) using HK-NYS-NHS-2. The resulting protein–DNA conjugates were purified by anion exchange chromatography (proFIRE®, Dynamic Biosensors GmbH), buffer-exchanged into HE40 (10 mM HEPES, 40 mM NaCl, 0.05% Tween-20, 50 μ M EDTA, 50 μ M EGTA), and stored at -80 °C.

Experiments were conducted on a heliX⁺ biosensor using a standard adapter chip (ADP-48-2-0, Dynamic Biosensors GmbH). The chip surface was functionalized with DNA ligands from the New Y-Structure kit (HK-NYS-1, Dynamic Biosensors GmbH). Spot 1 was functionalized with a pre-incubated mixture of Y-structure red and green adapter strands carrying the protein conjugates (LS1-CRBN^{mid}, LS2-Brd4^{BD2}), while spot 2 was functionalized with cAnchor 2. DNA ligands and protein conjugates were prepared according to the HK-NYS-1 user manual [5].

FRET kinetics experiments were performed and analysed in heliOS using the “Y-structure FRET kinetics – auto LED” assay (green LED: auto, red LED: off); FPS measurements were performed and analysed in heliOS, with green LED: off, red LED: auto. Association and dissociation rates (k_{on} , k_{off}) and equilibrium dissociation constants (K_d) were obtained from globally fitted single-exponential models with blank referencing. Association and dissociation times were 120 s and

200 s, respectively, at a flow rate of 200 $\mu\text{L}/\text{min}$ at 25 $^{\circ}\text{C}$. Rate scale plots (Figure 2) and kinetic rate maps (Figure 4) were generated in Origin (v9, OriginLab Corporation).

The biochip was regenerated with high-pH regeneration solution (SOL-REG-1-5, Dynamic Biosensors GmbH) and freshly functionalized before each concentration series.

Results and Discussion

To measure PROTAC-mediated ternary complex formation, both arms of the Y-structure were functionalized with proteins: the Brd4^{BD2} target-conjugate was hybridized to the green-dye arm, and either CRBN^{midi} or CRBN:DDB1 ligase-conjugate was hybridized to the red-dye arm. Fluorescence was selectively excited in the green channel, while emissions from both green and red channels were recorded simultaneously. Upon injection of the PROTAC analyte, red emission was observed, reflecting indirect excitation via green-to-red FRET as the Y-structure closes and the PROTAC interlinks the target and ligase proteins (see Figure 2, ARV825 in red, dBET6 in blue and dBET1 in green). When the PROTAC dissociates, the Y-structure arms separate, and fluorescence in both channels returns to baseline. The kinetics are well described by a global single-exponential model, with resulting rate constants and affinities summarized in Figure 2B, 4 and Table 1.

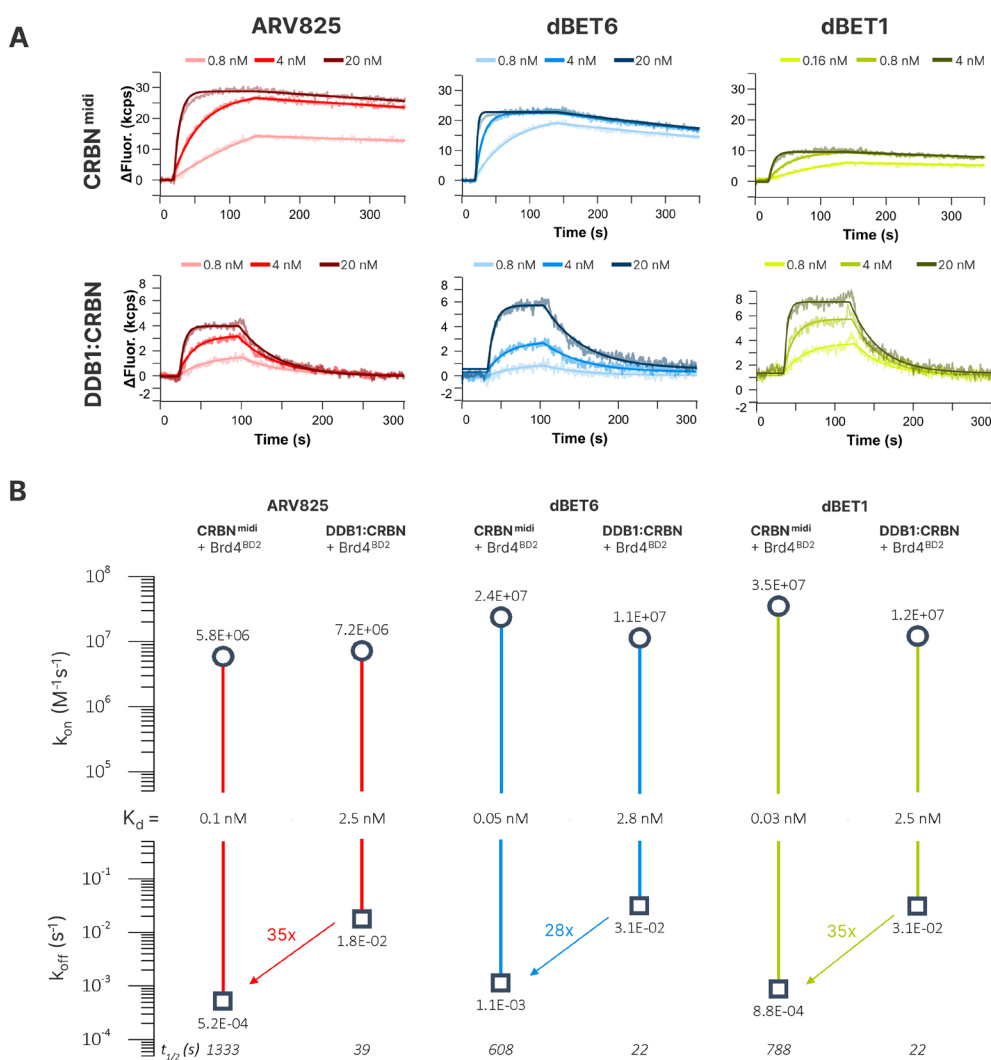


Figure 2. A) Kinetics of PROTAC-induced ternary complex formation between Brd4^{BD2} and CRBN^{midi} (upper panel) and DDB1:CRBN (lower panel). B) Kinetics of PROTAC-induced ternary complex formation with DDB1:CRBN and Brd4^{BD2}. The plots depict association and dissociation rates (k_{on} , k_{off}) and derived dissociation constants (K_{d}). Kinetic sensorgrams and scale plots are representing 3 different PROTACs, namely ARV825 (left, red), dBET6 (center, blue), dBET1 (right, green).

Comparison of ternary complex kinetics for ARV825 binding to Brd4^{BD2} with either CRBN^{mid} or DDB1:CRBN reveals pronounced differences. While the association rates are similar ($k_{on} = 5.83 \times 10^6 \text{ M}^{-1}\text{s}^{-1}$ for CRBN^{mid} vs. $7.20 \times 10^6 \text{ M}^{-1}\text{s}^{-1}$ for DDB1:CRBN), dissociation is markedly slower with CRBN^{mid} ($k_{off} = 0.52 \times 10^{-3} \text{ s}^{-1}$) compared to DDB1:CRBN ($k_{off} = 17.8 \times 10^{-3} \text{ s}^{-1}$), which returns to baseline within minutes. This 35-fold difference is reflected in the ternary complex half-lives: ~1333 s (~22 min) for CRBN^{mid} versus 39 s for DDB1:CRBN. Consequently, the equilibrium affinities differ by orders of magnitude, with CRBN^{mid} complexes in the picomolar range and DDB1:CRBN in the single-digit nanomolar range. A similar trend is observed for dBET6-induced ternary complex formation with Brd4^{BD2} and either CRBN^{mid} or DDB1:CRBN. The association rates are similar for both constructs ($k_{on} = 23.7 \times 10^6 \text{ M}^{-1}\text{s}^{-1}$ vs. $11.3 \times 10^6 \text{ M}^{-1}\text{s}^{-1}$), while the dissociation is about 28-fold slower in the presence of CRBN^{mid} ($k_{off} = 1.14 \times 10^{-3} \text{ s}^{-1}$ vs. $31.3 \times 10^{-3} \text{ s}^{-1}$). As for ARV825, this translates into half-lives of 608 s (~10 min) for the CRBN^{mid} complex and 22s for the DDB1:CRBN complex. The resulting affinities reflect this difference, with K_d values in the tens of picomolar range for CRBN^{mid} and single-digit nanomolar for DDB1:CRBN. Finally, dBET1-induced ternary complexes with Brd4^{BD2} and CRBN^{mid} form roughly three-fold faster than with DDB1:CRBN-complexes ($k_{on} = 34.9 \times 10^6 \text{ M}^{-1}\text{s}^{-1}$ vs. $12.1 \times 10^6 \text{ M}^{-1}\text{s}^{-1}$) and dissociate 3-fold slower ($k_{off} = 0.88 \times 10^{-3} \text{ s}^{-1}$ vs. $30.9 \times 10^{-3} \text{ s}^{-1}$), confirming the behaviour already observed with ARV825 and dBET6. Similarly to the other two PROTACs, the half-lives of dBET1-induced complexes are highly prolonged in presence of CRBN^{mid} (788 s, circa 13 minutes) than with DDB1:CRBN (22 s). Consequently, the complexes' dissociation constants differ by two orders of magnitude, yielding an affinity constant in the picomolar range for CRBN^{mid} and single-digit nanomolar for DDB1:CRBN, confirming the stabilization observed previously with ARV825 and dBET6. In addition, differences in the total red FRET fluorescence are observed for CRBN^{mid} across the different PROTACs. This signal is fully dependent on the size of the ternary complex and therefore on the distance achieved between the two dyes in the closed conformation.

We hypothesize that the enhanced stability of CRBN^{mid} ternary complexes arises from its sensor loop and the absence of DDB1. In the unbound, open conformation of full-length CRBN, the sensor loop (residues 341–361) interacts with DDB1 (residues 776–780), partially stabilizing the open state. Upon ligand binding CRBN adopts a closed conformation, whereby the sensor loop undergoes a large conformational rearrangement, forming a beta hairpin packed between the TBD and Lon domains, as illustrated by Watson et al. (4). In open CRBN^{mid}, the sensor loop is unbound due to the absence of DDB1, which may destabilize the open state relative to the full-length DDB1:CRBN complex. Consequently, the closed, ligand-bound conformation could be more favorable in CRBN^{mid}, as the sensor loop lacks its interaction partner and may preferentially adopt the closed state, leading to higher affinities.

Table 1. Kinetic binding rates and constants of PROTACs interacting with Brd4^{BD2} and CRBN^{mid} or DDB1:CRBN [3] on the Y-structure. Values shown represent the mean from at least two independent experiments.

PROTAC	E3 LIGASE	Target (POI)	Interaction	k_{on} ($E6 \text{ M}^{-1}\text{s}^{-1}$)	k_{off} ($E-3 \text{ s}^{-1}$)	k_d (nM)	$t_{1/2}$ (s)
ARV825	CRBN ^{mid}	Brd4 ^{BD2}	ternary	5.83	0.52	0.09	1333
	DDB1:CRBN	Brd4 ^{BD2}	ternary	7.20	17.8	2.47	39
	CRBN ^{mid}		binary	2.28	1.64	0.72	423
	DDB1:CRBN		binary	0.59	79	138	9
dBET6	CRBN ^{mid}	Brd4 ^{BD2}	ternary	23.7	1.14	0.05	608
	DDB1:CRBN	Brd4 ^{BD2}	ternary	11.3	31.3	2.77	22
	CRBN ^{mid}		binary	5.51	2.79	0.51	248
	DDB1:CRBN		binary	0.47	48.7	104	14
dBET1	CRBN ^{mid}	Brd4 ^{BD2}	ternary	34.9	0.88	0.03	788
	DDB1:CRBN	Brd4 ^{BD2}	ternary	12.1	30.9	2.55	22
	CRBN ^{mid}		binary	15.8	5.66	0.36	122
	DDB1:CRBN		binary	4.35	85.9	19.7	8

Additionally, binary interactions of the three PROTACs were also measured with CRBN^{mid} and DDB1:CRBN (3), in the absence of Brd4^{BD2} on the green arm (Figure 3, values listed in Table 1). Interestingly, the binary association rates with CRBN^{mid} are faster (4-times for ARV825 and dBET1, and 12-times for dBET6) than with full-length CRBN. While the dissociation rates are significantly slower (50-fold for ARV825, 18-fold for dBET6 and 15-fold for dBET1), consistently with what has been observed for the ternary kinetics.

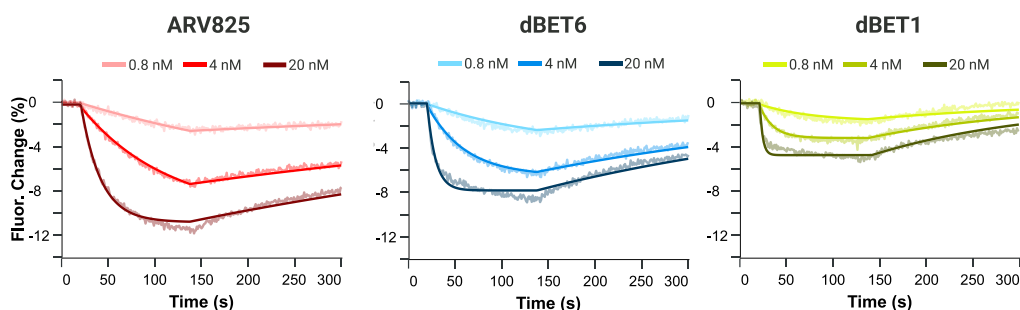


Figure 3. Binary kinetics of PROTACs with CRBN^{mid}. ARV825 (left, red traces), dBET6 (center, blue traces), dBET1 (right, green traces). PROTACs were injected at the specified concentrations, and fluorescence change upon PROTAC binary binding was recorded over time.

In conclusion, the iso-affinity kinetic plots shown in Figure 4 illustrates the kinetic differences between ternary and binary PROTAC interactions. Ternary complexes involving CRBN^{mid} display comparable association rates but significantly slower dissociation than those formed with DDB1:CRBN. Similarly, the binary interactions of the three PROTACs with CRBN^{mid} exhibit faster association rates and notably slower dissociation rates compared to their interactions with DDB1:CRBN. Although absolute kinetic values and K_d measurements differ, the overall trends are relatively consistent, indicating that CRBN^{mid} preserves the relative ranking of PROTACs and could reliably guide degraders selection.

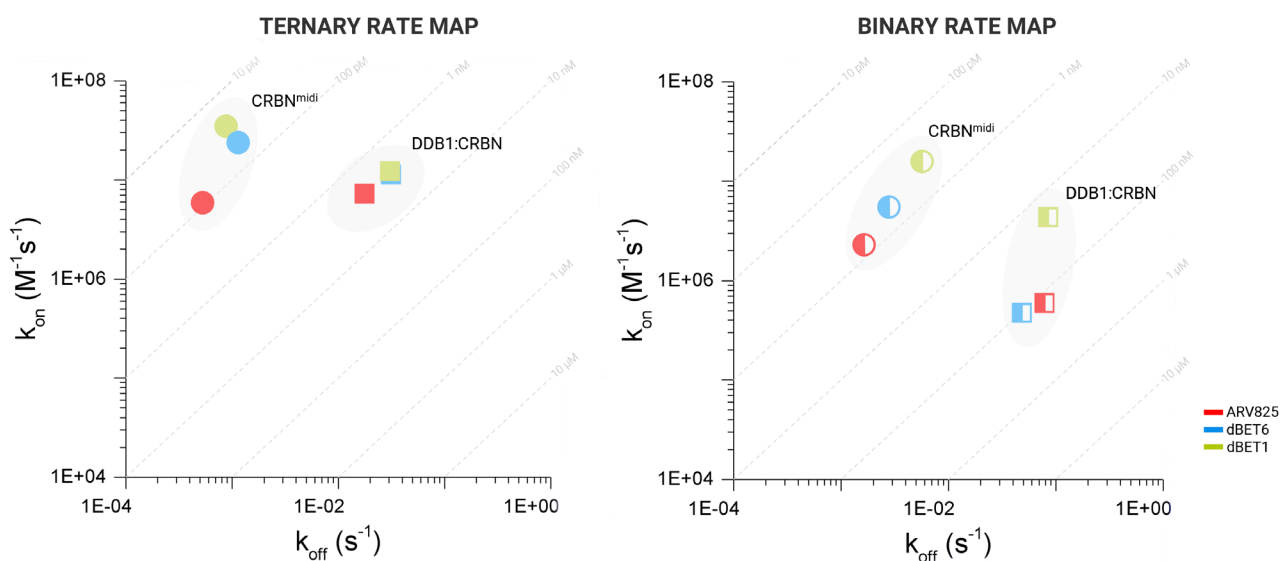


Figure 4. Rate maps for ternary and binary kinetics. Mean k_{on} rates are plotted versus mean k_{off} rates, the dashed iso-affinity lines are plotted from $K_d = 10$ pM to 10 μ M. Ternary rate constants are full symbols, binary rate constants are half full symbols. Circles represents kinetics with CRBN^{mid} as E3 ligase, while square symbols represents kinetics with DDB1:CRBN construct.

Conclusion

In this study, we compared CRBN^{mid}—a more stable and soluble variant of full-length CRBN developed by the Ciulli lab—against DDB1:CRBN to investigate PROTAC kinetics using the **heliX+** biosensor. Our results show that PROTAC interactions with CRBN^{mid} display pronounced differences in binding kinetics and affinity compared with the full-length DDB1:CRBN complex, most notably in dissociation rates and ternary complex half-lives. However, the overall trends remain consistent, demonstrating that CRBN^{mid} preserves the relative ranking of PROTACs and can reliably guide degrader selection.

Importantly, we highlight the Y-structure proximity assay as a powerful and accessible platform for degrader research, uniquely capable of resolving ternary complex kinetics without pre-incubation steps. By providing detailed mechanistic insights in a streamlined format, this approach has strong potential to accelerate PROTAC discovery and design optimization, offering a high-information assay for the early-stage characterization of PROTACs and in general all chemical inducers of proximity.

References

- [1] Kong, N. R.; Jones, L. H. Clinical Translation of Targeted Protein Degraders. *Clin. Pharmacol. Ther.* 2023, 114 (3), 558–568. doi.org/10.1002/cpt.2985.
- [2] Kroupova, A.; Spiteri, V. A.; Rutter, Z. J.; Furihata, H.; Darren, D.; Ramachandran, S.; Chakraborti, S.; Haubrich, K.; Pethe, J.; Gonzales, D.; Wijaya, A. J.; Rodriguez-Rios, M.; Sturbaut, M.; Lynch, D. M.; Farnaby, W.; Nakasone, M. A.; Zollman, D.; Ciulli, A. Design of a Cereblon Construct for Crystallographic and Biophysical Studies of Protein Degraders. *Nat. Commun.* 2024, 15 (1). doi.org/10.1038/s41467-024-52871-9.
- [3] Ponzio, I.; Solda, A.; Crowe, C.; Dahl, G.; Geschwindner, S.; Ciulli, A.; Rant, U. Proximity Biosensor Assay for PROTAC Ternary Complex Analysis. *ChemRxiv* March 6, 2024. doi.org/10.26434/chemrxiv-2024-8w4zb.
- [4] Watson, E.R., Novick, S., Matyskiela, M.E., Chamberlain, P.P., H de la Peña A., Zhu, J., Tran, E., Griffin, P.R., Wertz, I.E., Lander, G.C. Molecular glue CELMoD compounds are regulators of cereblon conformation. *Science*. 2022 Nov 4;378(6619):549-553. doi: 10.1126/science.add7574.
- [5] <https://shop.dynamic-biosensors.com/shop/reagents/helix-reagents/adapter-kits/y-structure-2-0-kit-1/>

Bruker Daltonics is continually improving its products and reserves the right to change specifications without notice. © Bruker Daltonics 01-2026, helix-1, 1925149

For Research Use Only. Not for use in clinical diagnostic procedures.

Bruker Switzerland AG

Fällanden · Switzerland
Phone +41 44 825 91 11

Bruker Scientific LLC

Billerica, MA · USA
Phone +1 (978) 663-3660

